

Source-rupture process of the 2011 Ibaraki-oki, Japan, earthquake (M_w 7.9) estimated from the joint inversion of strong-motion and GPS Data: Relationship with seamount and Philippine Sea Plate

Hisahiko Kubo,¹ Kimiyuki Asano,¹ and Tomotaka Iwata¹

Received 1 April 2013; revised 6 May 2013; accepted 10 May 2013; published 20 June 2013.

[1] The source-rupture process of the 2011 Ibaraki-oki earthquake was estimated from the joint inversion of the strong-motion and global positioning system (GPS) data. The estimated seismic moment and maximum slip are 7.8×10^{20} Nm (M_w 7.9) and 6.3 m, respectively. The total rupture duration is approximately 30 s. The derived source model has one large slip area, which is surrounded by the subducted seamount and the northeastern edge of the Philippine Sea plate. From this model, we concluded that the rupture propagation of the 2011 Ibaraki-oki earthquake was stopped by the seamount and the Philippine Sea plate. We also showed the possibility of the rupture of this event being the reactivation of the preexisting asperity of an event that occurred in 1923. **Citation:** Kubo, H., K. Asano, and T. Iwata (2013), Source-rupture process of the 2011 Ibaraki-oki, Japan, earthquake (M_w 7.9) estimated from the joint inversion of strong-motion and GPS Data: Relationship with seamount and Philippine Sea Plate, *Geophys. Res. Lett.*, 40, 3003–3007, doi:10.1002/grl.50558.

1. Introduction

[2] The 2011 Ibaraki-oki earthquake (M_{JMA} 7.6) occurred off the east coast of Ibaraki prefecture, Kanto, in the southeastern part of Japan at 15:15 on 11 March 2011, Japan Standard Time (JST; 06:15 on 11 March coordinated universal time). The moment magnitude (M_w) estimated from the centroid moment tensor (CMT) inversion by the Global CMT Project (GCMT) is 7.9. According to seismic information such as the source mechanism and hypocenter, this event is a thrust-type interplate earthquake at the subduction zone, where the Pacific plate (PAC) subducts beneath the North American plate (NA). It is the largest aftershock of the 2011 Tohoku earthquake (M_w 9.1) that occurred approximately 30 min before this event.

[3] At approximately 70 km east-southeast from the epicenter of the 2011 Ibaraki-oki earthquake, Mochizuki *et al.* [2008] found a subducting seamount by an active-source seismic survey using ocean-bottom seismometers (Figure 1a). In addition, the plate overlying PAC changes from NA in the north off Kanto to the Philippine Sea plate (PHS) in the south. Uchida *et al.* [2009] estimated the border between the two overlying plates (northeastern limit of the

PHS) based on the slip vectors of many interplate events (Figure 1a). The seamount has been considered to have a significant effect on the fault rupture, and numerous studies have focused on this topic [e.g., Scholz and Small, 1997; Mochizuki *et al.*, 2008]; however, few studies have clarified the role played by the seamount during fault rupture. In addition, the relationship between the fault rupture of an interplate earthquake and another nearby plate has attracted little attention. In this light, the analysis of the 2011 Ibaraki-oki earthquake presents a good opportunity to understand how the seamount and other plates affect the fault rupture of an interplate earthquake.

[4] In this study, we investigate the kinematic source-rupture process of the 2011 Ibaraki-oki earthquake by jointly analyzing the near-source strong ground motion and global positioning system (GPS) data. Then, we discuss the relationship of the derived source-rupture process with the seamount and PHS. We also discuss the relationship between this event and previous interplate earthquakes that have occurred around the source area.

2. Source Inversion Method

[5] For source inversion, we assumed a single planar fault model. The assumed fault plane is 120 km along strike \times 120 km along dip. The fault plane is divided into 144 subfaults of 10 km \times 10 km. The strike and dip angles of the fault plane are assumed to be 206° and 10°, respectively, with reference to the spatial distribution of earthquakes around the source area of this event as deduced from ocean-bottom seismographic observations [Yamada *et al.*, 2011]. The horizontal location of the rupture starting point is fixed at (141.2525°E, 36.1208°N), which is the epicenter location specified in the Japan Meteorological Agency (JMA) unified catalog. The depth of the rupture starting point is set to be 25 km, again with reference to the results reported in Yamada *et al.* [2011].

[6] For strong-motion data, we use three components of time series data from the 17 stations (11 KiK-net [Aoi *et al.*, 2000] stations observed at the borehole, four K-NET [Kinoshita, 1998] stations observed on the ground surface, and one F-net [Fukuyama *et al.*, 1998] station observed in the vault) (Figure S1a). Although the observed waveforms are expected to be contaminated with signals from other aftershocks, these signals can be neglected compared to the signal of the 2011 Ibaraki-oki earthquake in the analysis period band. Except for F-net station YMZ, whose original data is the velocity waveform, the observed acceleration waveforms were numerically integrated into velocity in the time domain. The velocity waveforms were band pass filtered from 5 to 50 s and resampled with a

Additional supporting information may be found in the online version of this article.

¹Disaster Prevention Research Institute, Kyoto University, Uji, Kyoto, Japan.

Corresponding author: H. Kubo, Disaster Prevention Research Institute, Kyoto University, Gokasho, Uji, Kyoto 611-0011, Japan. (kubo.hisahiko.26a@st.kyoto-u.ac.jp)

©2013. American Geophysical Union. All Rights Reserved.
0094-8276/13/10.1002/grl.50558

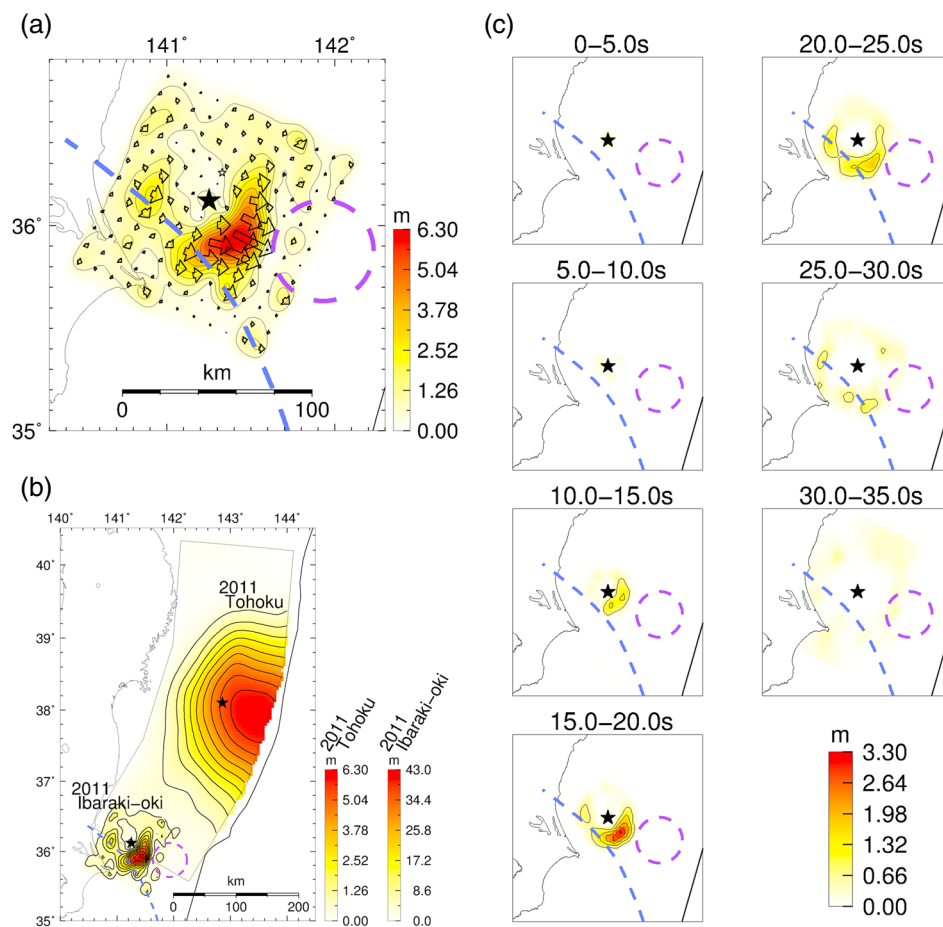


Figure 1. (a) Slip distribution projected on the map. The arrows indicate the slip direction of the hanging wall relative to the foot wall. The solid star indicates the rupture starting point. The blue broken line indicates the northeastern edge of the Philippine Sea plate [Uchida *et al.*, 2009]. The purple broken circle indicates the subducted seamount [Mochizuki *et al.*, 2008]. (b) Comparison of the slip distribution of the 2011 Ibaraki-oki earthquake with that of the 2011 Tohoku earthquake [Kubo and Kakehi, 2013]. (c) Snapshots of the rupture propagation at a time step of 5 s.

sampling interval of 0.5 s. The time length of the dataset in the source inversion is 50–80 s, which depends on the record length at each site (starting 10 s before S-wave arrival, which was carefully identified by visual inspection).

[7] We also use the GPS data recorded using the GPS Earth Observation Network (GEONET) [Sagiya *et al.*, 2000]. We obtained station positions at every 30 s using Kinematic Precise Point Positioning as implemented in RTKLIB Ver. 2.4.1 [Takasu, 2011]. To avoid the effect of the 2011 Tohoku earthquake, other aftershocks, and afterslip, the preseismic and postseismic positions were obtained by averaging the positions from 15:13:00 to 15:15:00 (JST) and those from 15:23:00 to 15:25:00 (JST), respectively. Then, the coseismic static displacements for this event were obtained by differencing these preseismic and postseismic positions. Two horizontal displacement components (east-west and north-south) at 83 GEONET stations are used in this study (Figure S1b).

[8] The strong-motion Green's functions were calculated using the discrete wave number method [Bouchon, 1981] and the reflection/transmission matrix method [Kennett and Kerry, 1979] assuming a one-dimensional underground velocity structure model. The one-dimensional underground velocity structure model was constructed for each station from Japan Integrated Velocity Structure Model Version 1 [Koketsu

et al., 2012]. The reliability of the strong-motion Green's functions is discussed in the supplement. As for the geodetic Green's function, we calculate the theoretical static displacements caused by a unit slip on each subfault assuming a homogeneous elastic half-space, as proposed in Okada [1992].

[9] The spatiotemporal rupture history is estimated by kinematic linear waveform inversion with multiple time windows [Hartzell and Heaton, 1983]. The slip time history of each subfault is represented by the superposition of seven time windows with 4.0 s width, each of which is put with 2.0 s lag. Thus, an allowed slip duration for each subfault is 16 s. The reason for adopting this value is that comparison between the results allowing the 16 s slip duration and more long slip duration indicates that the slip duration adopted in this study is sufficient to obtain a stable inversion result. The model parameters of the source inversion are the weights of the two orthogonal slip vectors given in each time window at each subfault. By giving a nonnegative constraint [Lawson and Hanson, 1974] to these weights, the rake angle of the slip vector of each subfault is allowed to vary within $90^\circ \pm 45^\circ$. The spatiotemporal smoothing constraint on slips was applied following the procedure proposed by Kubo and Kakehi [2013]. The first time window triggering velocity of 2.2 km/s was selected so as to minimize the residual of strong-motion data fitting.

[10] In many previous studies, the relative weights between different types of datasets and the weight of the smoothing constraint were selected based on the minimum Akaike's Bayesian Information Criterion [ABIC; Akaike, 1980] condition [e.g., Asano *et al.*, 2005]. In this study, however, we found that the source model obtained using the minimum ABIC condition showed poor fitting of static displacements and an overly large seismic moment compared to that estimated by GCMT. Therefore, these relative weights are determined by a trial-and-error process based on the following conditions: (1) both fittings of strong-motion waveforms and static displacements are good and (2) the estimated seismic moment is reasonable compared to that estimated by GMCT. It is noted that the source model obtained by using the minimum ABIC condition shows a similar trend of slip distribution to the one selected in this study (Figure S4). Yagi and Fukahata [2011a] claimed that reasonable results cannot be obtained by using the minimum ABIC condition when the modeling errors in Green's function are neglected. Fukuda and Johnson [2008] noted that the ABIC-based method with positivity constraints typically generates significantly undersmoothed or oversmoothed slip distributions. These studies may explain why the ABIC-based method did not work in this study.

3. Result

[11] Figure 1a shows a projection of the obtained slip distribution on the map. A large slip area (>3.15 m) is located approximately 20 km southeast of the hypocenter, and it is surrounded by the northeastern edge of the PHS and the subducted seamount. Its spatial extent is approximately $60 \text{ km} \times 30 \text{ km}$. The estimated seismic moment and the maximum slip are $7.8 \times 10^{20} \text{ Nm}$ (M_w 7.9) and 6.3 m, respectively. Figure 1b shows the slip distributions of both the 2011 Ibaraki-oki earthquake and the 2011 Tohoku earthquake (Kubo and Kakehi, 2013). The source area of the 2011 Ibaraki-oki earthquake does not overlap with the large coseismic slip area of the 2011 Tohoku earthquake. This relationship can be seen even when we refer to other source models of the 2011 Tohoku earthquake [e.g., Yagi and Fukahata, 2011b; Wei *et al.*, 2012]. Figure 1c shows snapshots of rupture propagation in time steps of 5 s. Figure S5 shows the slip rate function at each subfault. In the first 10 s, the rupture grows slowly in the vicinity of the hypocenter, and the slip amount is small. At 10 s, the rupture with large slip propagates toward the southeast, that is, the direction between the seamount and the northeastern limit of the PHS. From 15 s to 30 s, the rupture in the deep part propagates northeastward along the northeastern limit of the PHS. The total rupture duration is approximately 30 s. The derived source model demonstrates that the fault rupture of the 2011 Ibaraki-oki earthquake did not reach the seamount area and the PHS-PAC contact zone, indicating that the rupture propagation of this event was stopped by the seamount and PHS.

[12] Figure 2 shows a comparison of the final slip distribution with the spatial distribution of the interplate earthquakes before and after the 2011 Ibaraki-oki earthquake. In both periods, few interplate earthquakes occurred in the large slip area. In addition, no interplate earthquakes occurred in and around the subducted seamount in both periods. Figure 2b shows the afterslip area for 1 month after the 2011 Tohoku

earthquake [Ozawa *et al.*, 2012]. This area is located around the large slip area and is mostly found in the PHS-PAC contact zone. The fact that the epicenter distribution of the interplate aftershocks and the large afterslip area do not overlap the large coseismic slip area is consistent with observations made in past earthquakes [e.g., Ozawa *et al.*, 2004; Asano *et al.*, 2011].

[13] Figure S6 shows a comparison of the observed and the synthetic strong-motion velocity waveforms. The variance reduction of the strong-motion data is 84.4%. Figure S7 shows a comparison of the observed and the theoretical static displacements. The variance reduction and root mean squared deviation of GPS data are 97.4% and 0.055 m, respectively. The fitting in both data is quite good.

4. Discussion

[14] With regard to the relationship between the fault rupture and the seamount, the following two points were noted in this study: (1) the fault rupture of the 2011 Ibaraki-oki earthquake did not reach the seamount area and (2) no interplate earthquakes occurred in and around the subducted seamount before and after the 2011 Ibaraki-oki earthquake. Scholz and Small [1997] suggested that the subduction of a large seamount increases the normal stress across the subduction interface, and the seismic coupling between the subducted plate and the overriding plate becomes locally stronger. Accordingly, the seamount is expected to work as a rupture "barrier" if the seamount area is not ready for coseismic rupture. This could well explain our results regarding the relationship between the fault rupture and the seamount. This hypothesis suggests that a coseismic slip happened to not occur at the seamount area during the 2011 Ibaraki-oki earthquake and that there is a possibility that a large earthquake will occur at the seamount area in the future.

[15] Mochizuki *et al.* [2008] suggested that the interplate coupling at the seamount area is very weak probably because of fluid-rich sediment entrained with the subducted seamount. This could also explain our results, and therefore, we cannot rule out this possibility. For judging which interpretation is better, it is necessary to investigate the interplate coupling at the seamount area. Some studies estimated the interplate coupling on the subduction boundary using the inland GPS data [e.g., Loveless and Meade, 2010], and they did not find strong coupling at the seamount area. However, as shown in the appendix of Nishimura *et al.* [2004], the inland GPS data have very limited resolving power for offshore fault slips on the subduction boundary, and hence, it is possible that the strong coupling at the seamount area was not identified by previous studies using inland GPS data. Other studies estimated the interplate coupling using small repeating earthquakes [e.g., Uchida *et al.*, 2009]. However, this method is unsuitable for estimating the interplate coupling at the seamount area because repeating earthquakes cannot occur at very strong or nearly zero coupling areas. Actually, no repeating earthquake identified by Uchida *et al.* [2009] occurred at the seamount area. Therefore, we cannot judge which interpretation is better from previous studies, and further study with a focus on interplate coupling at the seamount area will be required.

[16] Next, we focus on the relationship between fault rupture and PHS. Because NA is a continental plate and PHS is an oceanic plate, the condition in the PHS-PAC

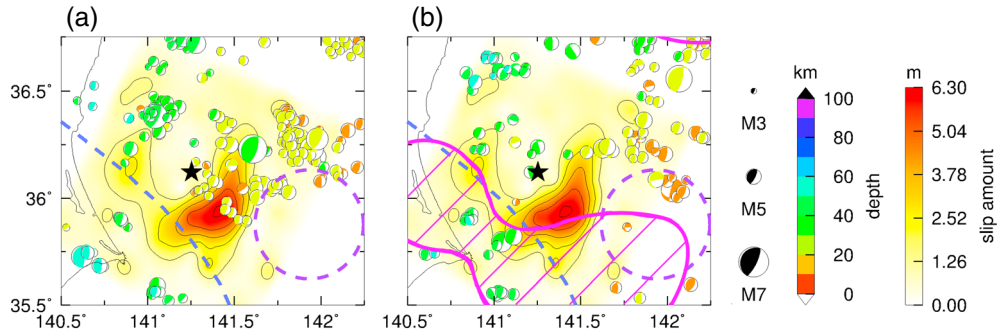


Figure 2. Map view of the final slip distribution compared with the spatial distribution of CMTs of the interplate earthquakes greater than M_w 3.0 in periods (a) 2001–2010 (before the off-Ibaraki earthquake in 2011) and (b) 11 March 15:15–11 April 15:15, 2011 (after the off-Ibaraki earthquake in 2011). These interplate earthquakes are selected from the F-net CMT solution catalog using the following conditions: $155^\circ \leq \text{strike } \phi \leq 245^\circ$; $0^\circ \leq \text{dip } \delta \leq 40^\circ$; $45^\circ \leq \text{rake } \lambda \leq 135^\circ$. The size of the CMTs is proportional to its moment magnitude. The pink shaded zone in Figure 2b represents the area with afterslip over 0.4 m for 1 month after the 2011 Tohoku earthquake [Ozawa *et al.*, 2012].

contact zone appears to differ from that in the NA-PAC contact zone. For example, Uchida *et al.* [2009] estimated the interplate coupling coefficient from the cumulative slip of small repeating earthquakes and suggested that the coupling rate in the PHS-PAC contact zone is lower than that in the NA-PAC contact zone. In addition, a large afterslip mostly occurred in the PHS-PAC contact zone, as mentioned above. This observation and the weak interplate coupling in the PHS-PAC contact zone indicate that this zone would be the compliant area or velocity-strengthening fault area [Boatwright and Cocco, 1996; Matsuzawa, 2009]. Because of such differences between the conditions in the NA-PAC and PHS-PAC contact zones, the rupture in the NA-PAC contact zone cannot easily propagate through the PHS-PAC contact zone.

[17] In the off-Ibaraki region, characteristic large ($M \sim 7$) interplate earthquakes have occurred with a recurrence interval of approximately 20 years. Figure 3 shows a comparison of the estimated slip distribution of the 2011 Ibaraki-oki earthquake with the spatial earthquake distribution of $M \sim 7$ interplate events occurring off Ibaraki in the past. Although most earthquake sequences are located north or northwest of the large slip area of the 2011 Ibaraki-oki earthquake, the hypocenter of the earthquake (M_{JMA} 7.1) at 02:24 on 2 June 1923 (JST) is located in the large slip area of the 2011 Ibaraki-oki earthquake. Provided that this area had been completely coupled for 88 years before the 2011 Ibaraki-oki earthquake and that the PAC subducts westward beneath the NA at a rate of 8 cm/year [e.g., Loveless and Meade, 2010], the accumulated slip deficit at this area was expected

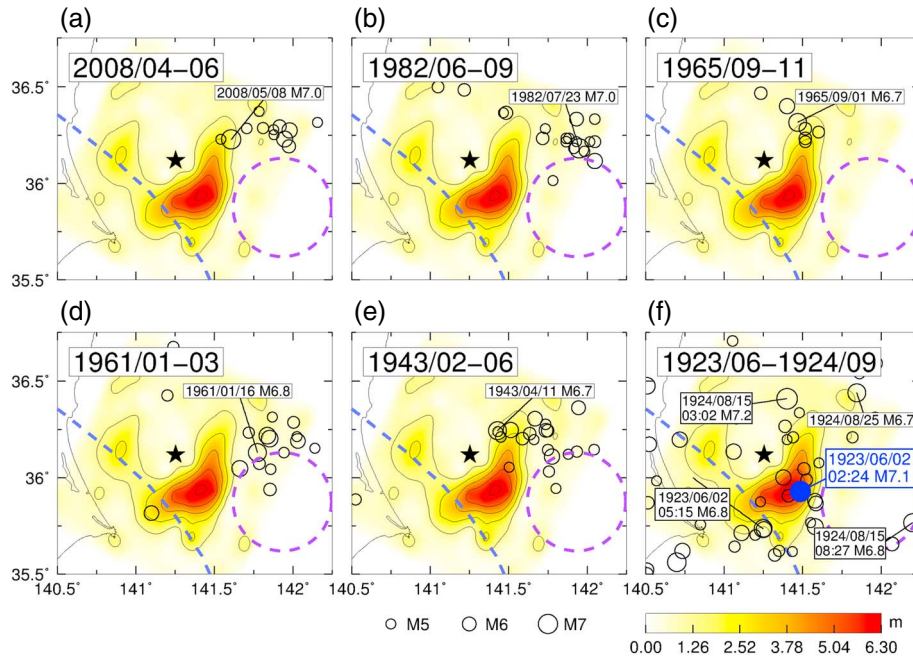


Figure 3. Map view of the final slip distribution compared with the source regions of interplate events that occurred in the off-Ibaraki region and are greater than M_{JMA} 5.0 in each period: (a) April to June 2008; (b) June to September 1982; (c) September to December 1965; (d) January to March 1961; (e) February to June 1943; and (f) June 1923 to September 1924. The size of the circle is proportional to its JMA magnitude (M_{JMA}). The earthquake that occurred at 2:24 on 2 June 1923 (JST) is drawn in blue for emphasis.

to be approximately 7 m. This value is comparable to the estimated maximum slip value of the 2011 Ibaraki-oki earthquake. This suggests the possibility that the rupture of the 2011 Ibaraki-oki earthquake is the reactivation of the preexisting asperity of the 1923 event, although the JMA magnitude (M_{JMA} 7.6) of the 2011 event is far larger than that of the 1923 event (M_{JMA} 7.1). This idea is also supported by the observation that few interplate earthquakes occurred in the large slip area of the 2011 Ibaraki-oki earthquake before this event (Figure 2a).

5. Conclusion

[18] The source-rupture process of the 2011 Ibaraki-oki earthquake was estimated from the joint inversion of strong-motion and GPS data. The derived source model demonstrates that the fault rupture of the 2011 Ibaraki-oki earthquake did not reach the seamount area and the PHS-PAC contact zone. This indicates that the rupture propagation of this event was stopped by the subducted seamount and PHS. This can be interpreted as follows: (1) the subducted seamount acts as a rupture barrier, and (2) because the PHS-PAC contact zone has low interplate coupling and is regarded as the compliant area, the rupture in the NA-PAC contact zone cannot easily propagate through the PHS-PAC contact zone. We also suggest the possibility that the rupture of this event is the reactivation of the preexisting asperity of an event that occurred in 1923.

[19] **Acknowledgments.** We thank the two anonymous reviewers for their helpful comment. We used the strong-motion data recorded by K-NET, KiK-net, and F-net of the National Research Institution for Earth Science and Disaster Prevention and the GPS data recorded by GEONET of the Geospatial Information Authority of Japan. We also used Generic mapping tools [Wessel and Smith, 1998] to draw the figures. This work is partially supported by the Observation and Research Program for Prediction of Earthquakes and Volcanic Eruptions from the Ministry of Education, Culture, Sports, Science, and Technology (MEXT), Japan and by the Grant-in-Aid for Young Scientists (B) 22710172 from the Japan Society for the Promotion of Science.

References

- Akaike, H. (1980), Likelihood and the Bayes procedure, in *Bayesian Statistics*, edited by J. M. Bernardo, M. H. DeGroot, D. V. Lindley, and A. F. M. Smith, 143–166 pp., University Press, Valencia, Spain.
- Aoi, S., K. Obara, S. Hori, K. Kasahara, and Y. Okada (2000), New Japanese uphole/downhole strong-motion observation network: KiK-net, *Seismol. Res. Lett.*, **72**, 239.
- Asano, K., T. Iwata, and K. Irikura (2005), Estimation of source rupture process and strong ground motion simulation of the 2002 Denali, Alaska, earthquake, *Bull. Seismol. Soc. Am.*, **95**, 1701–1715.
- Asano, Y., T. Saito, Y. Ito, K. Shiomi, H. Hirose, T. Matsumoto, S. Aoi, S. Hori, and S. Sekiguchi (2011), Spatial distribution and focal mechanisms of aftershocks of the 2011 off the Pacific coast of Tohoku earthquake, *Earth Planets Space*, **63**, 669–673.
- Boatwright, J., and M. Cocco (1996), Frictional constraints on crustal faulting, *J. Geophys. Res.*, **101**, 13,895–13,909, doi:10.1029/96JB00405.
- Bouchon, M. (1981), A simple method to calculate Green's function for elastic layered media, *Bull. Seismol. Soc. Am.*, **71**, 959–971.
- Fukuda, J., and K. M. Johnson (2008), A fully Bayesian inversion for spatial distribution of fault slip with objective smoothing, *Bull. Seismol. Soc. Am.*, **98**, 1128–1146.
- Fukuyama, E., M. Ishida, D. S. Dreger, and H. Kawai (1998), Automated seismic moment tensor determination by using on-line broadband seismic waveforms, *J. Seismol. Soc. Japan 2nd ser.*, **51**, 149–156, (in Japanese with English abstract).
- Hartzell, S. H., and T. Heaton (1983), Inversion of strong ground motion and teleseismic waveform data for the fault rupture history of the 1979 Imperial Valley, California, earthquake, *Bull. Seismol. Soc. Am.*, **73**, 1553–1583.
- Kennett, B. L. N., and N. J. Kerry (1979), Seismic waves in a stratified half space, *Geophys. J. R. Astron. Soc.*, **57**, 557–583.
- Kinoshita, S. (1998), Kyoshin Net (K-NET), *Seismol. Res. Lett.*, **69**, 309–332.
- Koketsu, K., H. Miyake, and H. Suzuki (2012), Japan Integrated Velocity Structure Model Version 1, Paper No. 1773 presented at the 15th World Conference on Earthquake Engineering, Int. Assoc. for Earthquake Eng., Lisbon, 24–28 Sep.
- Kubo, H., and Y. Kakehi (2013), Source process of the 2011 Tohoku earthquake estimated from the joint inversion of teleseismic body waves and geodetic data including seafloor observation data: Source model with enhanced reliability by using objectively determined inversion settings, *Bull. Seismol. Soc. Am.*, **103**, 1195–1220.
- Lawson, C. L., and R. J. Hanson (1974), *Solving Least Squares Problems*, Prentice-Hall, Old Tappan, New Jersey, pp. 340.
- Loveless, J. P., and B. J. Meade (2010), Geodetic imaging of plate motions, slip rates, and partitioning of deformation in Japan, *J. Geophys. Res.*, **115**, B02410, doi:10.1029/2008JB006248.
- Matsuzawa, T. (2009), Interplate earthquakes and the asperity model, *J. Seismol. Soc. Japan 2nd ser.*, **61**, S347–S355 (in Japanese with English abstract).
- Mochizuki, K., T. Yamada, M. Shinohara, Y. Yamanaka, and T. Kanazawa (2008), Weak interplate coupling by seamounts and repeating M ~ 7 earthquakes, *Science*, **321**, 1194–1197, doi:10.1126/science.1160250.
- Nishimura, T., T. Hirasawa, S. Miyazaki, T. Sagiya, T. Tada, S. Miura, and K. Tanaka (2004), Temporal change of interplate coupling in northeastern Japan during 1995–2002 estimated from continuous GPS observations, *Geophys. J. Int.*, **157**, 901–916, doi:10.1111/j.1365-246X.2004.02159.x.
- Okada, Y. (1992), Internal deformation due to shear and tensile faults in a half-space, *Bull. Seismol. Soc. Am.*, **82**, 1018–1040.
- Ozawa, S., M. Kaidzu, M. Murakami, T. Imakiire, and Y. Hatanaka (2004), Coseismic and postseismic crustal deformation after the M_w 8 Tokachi-oki earthquake in Japan, *Earth Planets Space*, **56**, 675–680.
- Ozawa, S., T. Nishimura, H. Muneke, H. Suito, T. Kobayashi, M. Tobita, and T. Imakiire (2012), Preceding, coseismic, and postseismic slips of the 2011 Tohoku earthquake, Japan, *J. Geophys. Res.*, **117**, B07404, doi:10.1029/2011JB009120.
- Sagiya, T., S. Miyazaki, and T. Tada (2000), Continuous GPS array and present-day crustal deformation of Japan, *Pure Appl. Geophys.*, **157**, 2303–2322.
- Scholz, C. H., and C. Small (1997), The effect of seamount subduction on seismic coupling, *Geology*, **25**, 487–490, doi:10.1130/0091-7613(1997)025<0487:TEOSSO>2.3.CO;2.
- Takasu, T. (2011), RTKLIB: An Open Source Program Package for GNSS Positioning, <http://www.rtklib.com/>.
- Uchida, N., J. Nakajima, A. Hasegawa, and T. Matsuzawa (2009), What controls interplate coupling?: Evidence for abrupt change in coupling across a border between two overlying plates in the NE Japan subduction zone, *Earth Planet. Sci. Lett.*, **283**, 111–121, doi:10.1016/j.epsl.2009.04.003.
- Wei, S., R. Graves, D. Helmberger, J. P. Avouac, and J. Jiang (2012), Sources of shaking and flooding during the Tohoku-Oki earthquake: A mixture of rupture styles, *Earth Planet. Sci. Lett.*, **333–334**, 91–100.
- Wessel, P., and W. H. F. Smith (1998), New, improved version of Generic Mapping Tools released, *Eos. Trans. AGU*, **79**, 579.
- Yagi, Y., and Y. Fukahata (2011a), Introduction of uncertainty of Green's function into waveform inversion for seismic source processes, *Geophys. J. Int.*, **186**, 711–720, doi:10.1111/j.1365-246X.2011.05043.x.
- Yagi, Y., and Y. Fukahata (2011b), Rupture process of the 2011 Tohoku-oki earthquake and absolute elastic strain release, *Geophys. Res. Lett.*, **38**, L19307, doi:10.1029/2011GL048701.
- Yamada, T., K. Nakahigashi, A. Kuwano, K. Mochizuki, S. Sakai, M. Shinohara, R. Hino, Y. Murai, T. Takanami, and T. Kanazawa (2011), Spatial distribution of earthquakes off the east coast of the Kanto region along the Japan Trench deduced from ocean-bottom seismographic observations and their relations with the aftershock sequence of the 2011 off the Pacific coast of Tohoku earthquake, *Earth Planets Space*, **63**, 841–845.